Magnetically tunable selective reflection of light by heliconical cholesterics

S. M. Salili, J. Xiang, H. Wang, Q. Li, D. A. Paterson, J. M. D. Storey, C. T. Imrie, O. D. Lavrentovich, S. N. Sprunt, J. T. Gleeson, and A. Jákli

Phys. Rev. E **94**, 042705 — Published 21 October 2016

DOI: 10.1103/PhysRevE.94.042705

Magnetically Tunable Selective Reflection of Light by Heliconical Cholesterics

S. M. Salili[a], J. Xiang[a], H. Wang[a], Q. Li[a], D.A Paterson[b], J. M.D. Storey[b], C. T. Imrie[b],

O. D. Lavrentovich[a], S. N. Sprunt[c], J. T. Gleeson[c], A. Jákli[a,d*]

[a] *Chemical Physics Interdisciplinary Program & Liquid Crystal Institute, Kent State University, Kent, OH 44242, USA*

[b] *Department of Chemistry, University of Aberdeen, AB24 3UE Scotland, UK*

[c] *Department of Physics, Kent State University, Kent, OH 44242, USA*

[d]*Complex Fluid Group, Wigner Research Centre, Budapest, Hungary*

Abstract

We present studies of chiral nematic liquid crystals composed of flexible dimer molecules subject to large DC magnetic fields between 0 and 31T. We observe that these fields lead to selective reflection of light depending on temperature and magnetic field. The band of reflected wavelengths can be tuned from ultraviolet to beyond the IR-C band. A similar effect induced by electric fields has been presented previously, and was explained by a field-induced oblique-heliconical director deformation in accordance with early theoretical predictions. The use of magnetic field here instead of electric allows precise measurements of some material constants and hold promise for wireless tuning of selective reflection.

1. Introduction

Flexible bent-core dimeric liquid crystal molecules are reminiscent of *nunchaku* fighting sticks: two rigid rod-like arms linked by a flexible, alkyl chain. These materials have recently taken center stage in liquid crystal science due to their extraordinary physical and electro-optical properties and novel states of orientational order [1–16]. In particular, many dimers with an odd number of carbons in the alkyl chain exhibit a "twist-bend" nematic (N_{tb}) phase, which was predicted by Dozov [17] assuming a negative bend-elastic constant that promotes spontaneous director bend. Since a pure director bend cannot fill space continuously, it must couple to a spontaneous twist or splay. In the case of twist-bend coupling, the result is a heliconical director modulation, where the helical axis is the average optical axis of the medium.

Recent experiments verified the existence of the N_{tb} phase with a surprisingly short heliconical pitch of order 10 nm. [7,18,19] The temperature-variation of this nanoscale pitch ("pseudo-layers") results in a Helfrich-Hurault type buckling instability [20] causing optically observable stripes and/or elongated focal conics similar to smectic phases. However, the N_{tb} does not have the periodic density modulation like true, layered smectics. Most of the flexible dimers with N_{tb} phase also exhibit a higher temperature uniaxial nematic (*N*) phase.

The effect of chirality on the *N* phase of flexible bent-core dimers has been investigated recently both experimentally [21,22] and theoretically [23]. Experiments on chiral, asymmetric dimers indicate a sequence of up to seven distinct nematic phases. As the constituent molecules are intrinsically chiral, the highest-temperature mesophase is either the cholesteric phase (*N**) or one of the blue phases. Stable phases observed at lower temperatures are variants of modulated nematic phases with apparently much larger pitch than in achiral N_{tb} dimers [10]. The addition of chiral dopants to achiral dimers [24,25] with *N*-N_{tb} phase sequence results in a wide temperature range blue phase even at low concentrations. Interestingly, the chiral dopant-induced helical structure in the *N** phase is expelled upon cooling to the N_{tb}* phase.

Depending on chiral dopant concentration, spontaneous formation of different stripe textures occurs in the *N** phase above N_{tb}. This phenomenon has been explained as a consequence of the bend elastic constant K_3 being sufficiently smaller than the twist constant K_2 ($K_2/K_3 > 2$). [26] Theoretically it was predicted almost 50 years ago by Meyer [27] and deGennes [28] that chiral *N** materials with $K_3 < K_2$ should have very distinct responses to external influences. While in conventional *N** state, where $K_3 > K_2$, the helix axis is perpendicular to $\vec{n}$, in case of $K_3 < K_2$, the helix axis makes an acute angle with to the director above a certain electric or magnetic threshold field. Experimentally Xiang et al has demonstrated the existence of such a heliconical state by using electric fields [14,15]. In mixtures containing odd-numbered flexible dimers they demonstrated selective reflection of light between 400 nm and 1000 nm. However, because of finite polarizability and conductivity, as well as the need to use conducting electrodes, the effects caused by electric fields on liquid crystals are substantially more complex than those caused by magnetic fields. Therefore, it is desirable to study the magnetic analog of the electrically-induced selective reflection effect, which we present here.

2. Experiments

The molecular structures of the liquid crystal materials used are shown in Figure 1(a). The rod-shaped compound, pentyl cyanobiphenyl (5CB) has a nematic phase between 21ºC and 35.5ºC. It has the same core structure as the arms of the two, symmetric dimers LCs 1-(4-cyanobiphenyl- 4′-yl)-6-(4-cyanobiphenyl-4′-yloxy) hexane (CB7CB) and 1″,9″-bis(4-cyanobiphenyl-4′-yl) nonane (CB9CB). On cooling from the isotropic phase, CB7CB forms a uniaxial nematic phase at 116ºC and then transitions to a twist-bend nematic phase at 103ºC. [29]. CB9CB exhibits the phase sequence *I* (122.4ºC) *N* (104.9ºC) N_{tb} (40.5ºC) Cr. The left-handed chiral dopant S811 (Merck) was added to the above materials to make two chiral mixtures, *M1* and *M2*. The composition of *M1* is *45:20:32:3 wt% 5CB:CB9CB:CB7CB:S811*, and its phase sequence is Iso (64.8℃) N* (30.0℃) N_{tb}*. The corresponding properties of *M2* are *44:20:32:4 wt % 5CB:CB9CB:CB7CB:S811* composition and Iso (65.0℃) N* (32.0℃) N_{tb}* phase sequence. The helical pitch of M1 and M2 at 35ºC and B=0 are p_o~ 4μm and p_o ~ 3μm, respectively.

Magneto-optical experiments were carried out in the split-helix, resistive, solenoid magnet at the National High Magnetic Field Laboratory (NHMFL) [30]. The mixtures were loaded in $10 \times 10\ mm$ planar glass cells, whose inner surfaces are treated with a unidirectionally rubbed polyimide PI2555 (HD Micro Systems) that promotes molecular alignment parallel to the substrates (planar alignment) and along the rubbing direction. The separation d between substrates was $30\ \mu m$. Each filled liquid crystal cell is inserted into a Teflon-insulated, temperature-controlled oven (temperature stability ± 0.05℃) with optical access parallel to the magnetic field direction. Two high-precision temperature sensors are embedded in the oven, one is a glass-encapsulated thermistor and the other a platinum resistive temperature device. Neither showed any drift during application of high magnetic fields. The oven is inserted into the magnet bore and positioned 5cm above the center line where the maximum achievable field is 31T.

Optical measurements were carried out with the optical path oriented parallel to the field and to the heliconical axis of the sample. A standard optical spectroscopy setup (see Figure 1(b)), incorporating a non-polarized tungsten halogen light source (Ocean Optics LS-1) and visible/infrared spectrometers (Ocean Optics USB2000 and NIRQUEST), was used to measure the intensity spectrum of the reflected light as a function of wavelength from 400 nm to 1700

nm. The reflectance is the ratio of the reflected intensity from the LC cell and from a mirror. The background intensity was deducted by using a matt black surface representing the zero level.

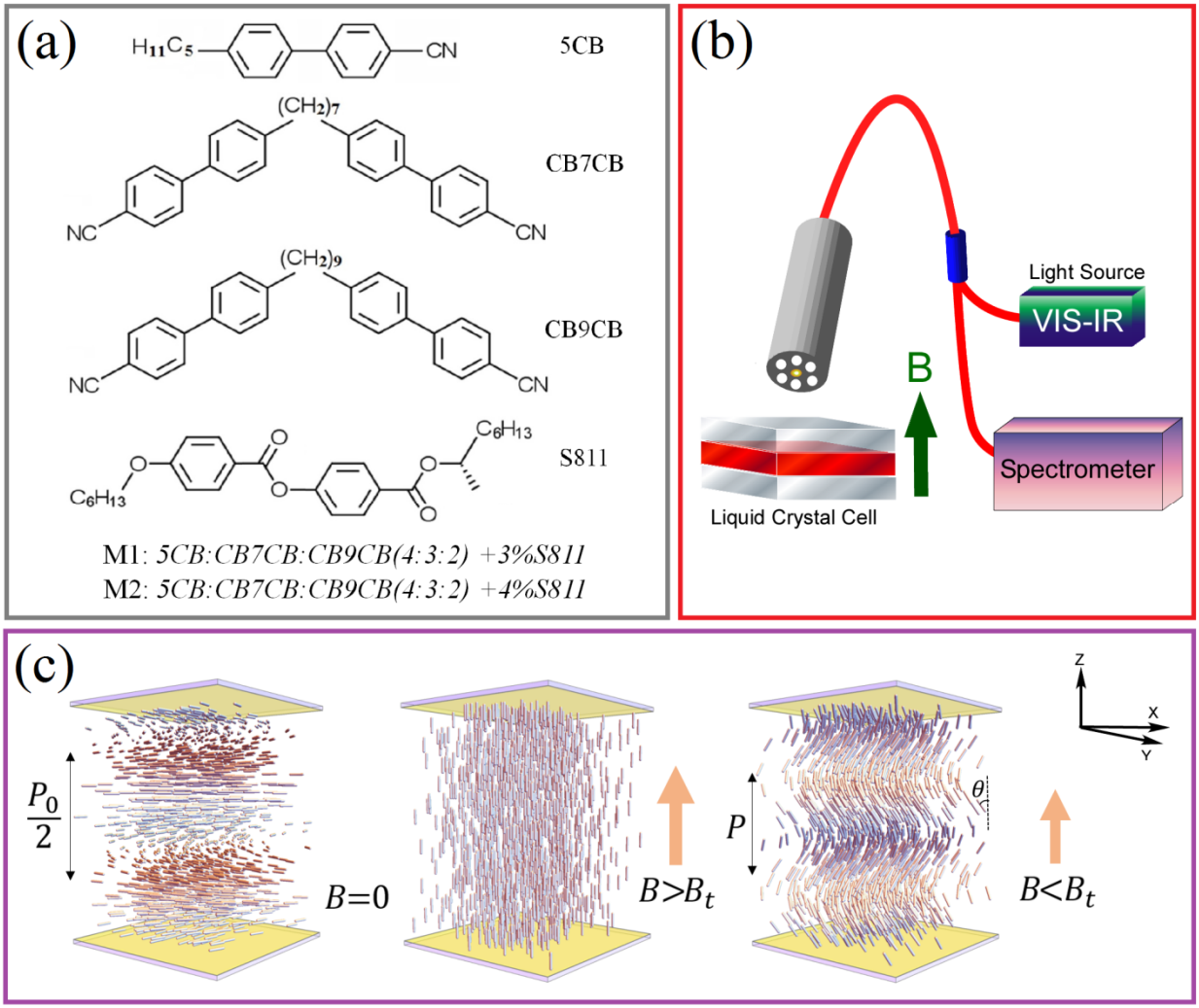

Figure 1: (a) Molecular structures of the components and their composition used in the studied mixtures M1 and M2; (b) Schematic of the experimental setup for measurement of optical reflection spectra in an applied magnetic field; (c) Illustration of the director profile of the liquid crystal at zero magnetic field (left), at high magnetic field that aligns the director uniformly along the magnetic field (middle), and at magnetic field below a threshold that creates heliconical structure.

Prior to each reflection measurements, the samples were heated to the isotropic phase, and cooled (at 0T) at 1ºC/min until the desired temperature within the N* phase is reached. The director structure of this initial alignment is shown in the left hand side of Figure 1(c). The helix

axis is normal to the substrates and has a pitch p_o. The magnetic field was then increased (at 5T/min) to 31 T, and maintained for 3 minutes. This field was enough to unwind the helix and rotate the director along them magnetic field as shown in the middle of Figure 1(c). The field was then decreased (5T/min) to various levels, and kept constant at each level for 3 minutes before the reflection spectrum was recorded. When the field was smaller than a threshold B_t, a heliconical director structure forms with a pitch p being different from p_o of the initial N^* structure. This is shown schematically on the right hand side of Figure 1 (c).

3. Results

Figure 2 presents reflection spectra for the mixture *M1* for various magnetic field levels and for three different temperatures in the N^* range. The peaks could be well fitted by Lorentzian distribution.

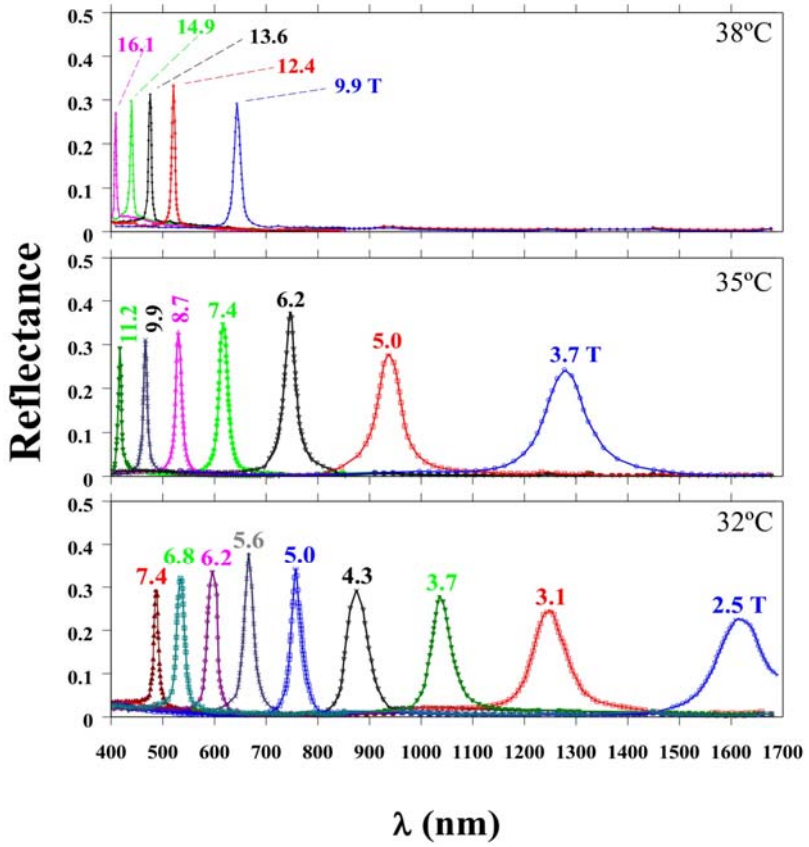

Figure 2: Reflection spectra recorded from the M1 mixture for different values of the magnetic fields at temperatures of 32℃ (bottom), 35℃ *(middle) and* 38℃ (top)*; all are within the N* range.*

As one can see, decreasing the field leads to a shift of the reflection spectrum toward the IR. At 38°C, a sharp reflection appears first at B_1=16.1T with peak position at 410 nm. When the field is stepped down to 9.9 T, the peak shifts to 650 nm. Below 9.9 T, it disappears. At lower temperatures, the onset of selective reflection occurs at lower fields (e.g., B_1 (35ºC) = 11.2 T and B_1 (32ºC) = 7.4 T), and the peak position shifts over a broader range with decreasing field levels, before eventually disappearing at low field. In particular, at 35ºC, selective reflection spans the range 420 to 1300 nm for field levels between 11.2 and 3.7 T. At 32°C, the span ranges from 450 to 1600 nm for fields between 7.4 and 2.5T, and reaches notably further into the IR. Below 2.5 T the peak shifts outside the limit of our spectrophotometer (λ_{max} =1700nm), so the tunable wavelength certainly exceeds 1700 nm. We note that in this range, the field necessary to induce tuning approaches that achievable with permanent magnets. At all temperatures, the width of the reflection peak increases as the peak wavelength increases.

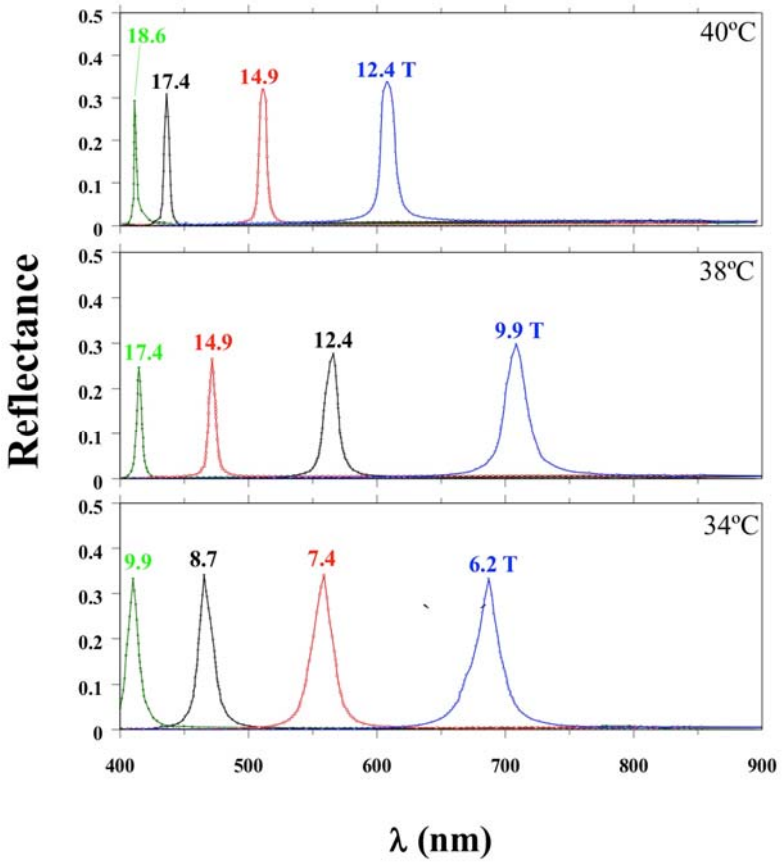

Figure 3: Reflection spectra recorded from the M2 mixture for various magnetic fields at temperature of 34°C, 38°C *and* 40°C.

Figure 3 presents reflection spectra for the *M2* mixture at various fields and for different temperatures. The characteristics of the spectra are similar to those for *M1*, except that for *M2* the reflection band is limited to the visible range. As seen for *M1*, the field level for onset of selective reflection in *M2* decreases with decreasing temperature (B_1(40ºC)=18.6T, B_1(38ºC)=17.4T, B_1(36ºC)=13.6T and B_1(34ºC)=9.9T), and decreasing the field shifts the reflection to higher peak wavelength and larger width.

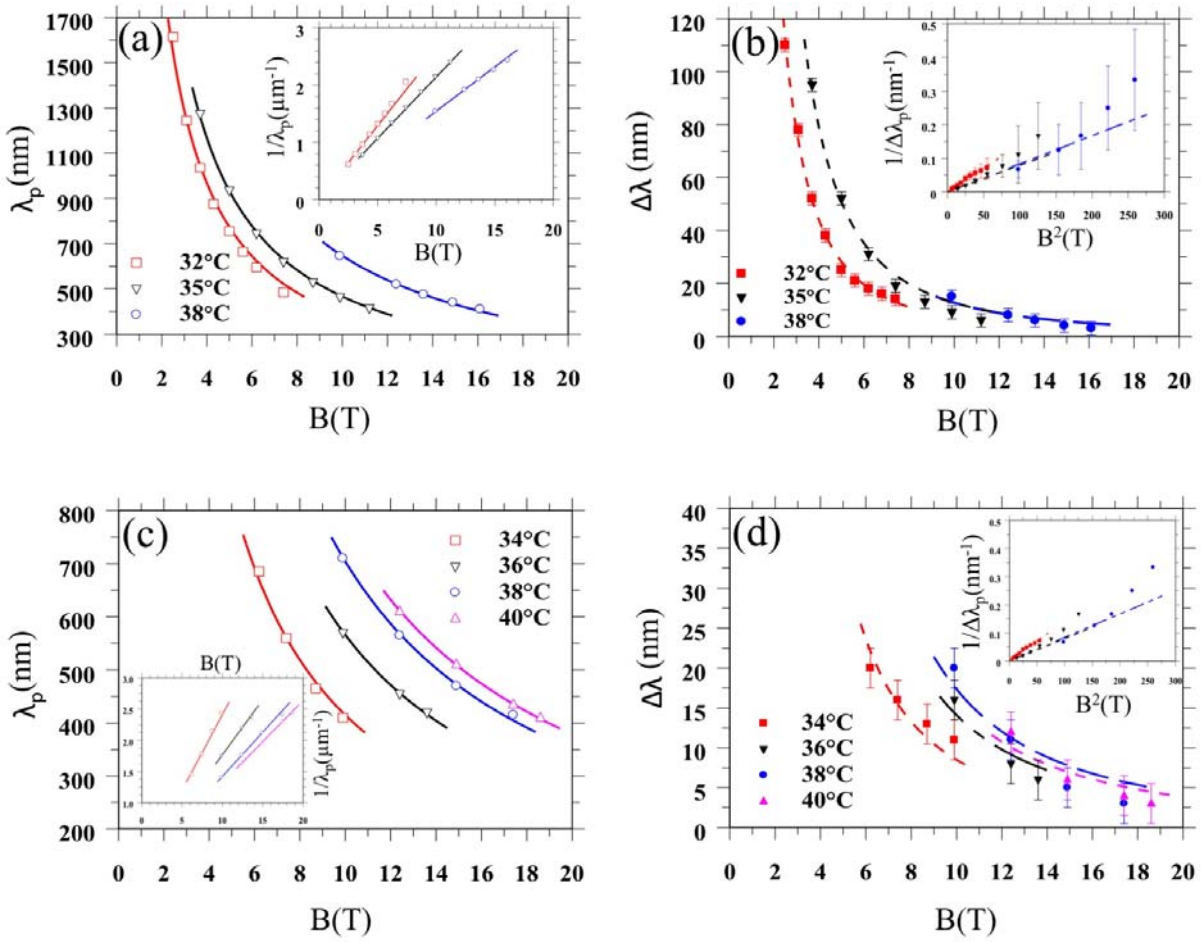

Figure 4: Magnetic field dependence of the wavelength and full width at half maximum (FWHM) of the selective reflection peak observed at different temperatures. (a) λp(B) (inset 1/λp(B)) for M1, (b) Δλ(B) (inset 1/Δλ(B²)) for M1, (c)) λp(B) (inset 1/λp(B)) for M2 and (d) Δλ(B) (inset 1/Δλ(B²)) for M2.

The magnetic field dependences of the peak positions (λ_p) and the full width at half maximum ($\Delta\lambda$) at various temperatures are plotted in Figure 4(a) and (b) for *M1* and Figure 4(c)

and (d) for *M2*. For both materials and at all measured temperatures, we fit the peak positions and widths to the following forms: $\lambda_p(B) = a(T)/B$ and $\Delta\lambda(B) = b(T)/B^2$. The fitted values of the parameters a and b are the following: For M_1: *a(32ºC)=3867, a(35ºC)=4666, a(38ºC)=6465* in units of nm·T; *b(32ºC)=703*, *b(35ºC)=1265, b(38ºC)*=1267 in units of nm·T^2. For M_2: *a(34ºC)=4152, a(36ºC)=5660, a(38ºC)=7044*; *a(40ºC)=7585; b(34ºC)=851*, *b(36ºC)=1410, b(38ºC)=1734, b(40ºC)=1551.* The fit for peak position describes our data slightly better than that for peak width.

As the peak positions depend both on the magnetic field and temperature, one can also tune the spectra by fixing the magnetic field and varying the temperature. For example, for *M1* at *B=7.4T* the peak can be shifted from *450 nm* to *950 nm* by heating the sample from *32ºC* to *39ºC*. Both λ_p and $\Delta\lambda$ increase with temperature, the former linearly with *T* and the latter approximately so.

Although the height of the reflected peaks shows non-monotonous behavior, the area *A* under the peaks increases with λ_p as $A = \alpha \cdot \left(\lambda_p - \lambda_o\right)$. The fitted parameters are $\alpha \simeq 0.02 - 0.025$ (when the transmittance is normalized to 1) for both materials (indicating that only 2-3% of the total light intensity is reflected), and $\lambda_o \simeq 250nm$ for *M1* and $\lambda_o \simeq 350nm$ for *M2*. These latter values can be considered as the lower limit of the selective reflection and show that they start in the *UV* range. Unfortunately, we could not follow the peaks in the UV range due to the spectral limitations of our light source and the absorption of the glass substrates.

4. Discussion

The magnetic field induced director deformation of a chiral nematic liquid crystal can be described by using the Frank-Oseen free energy functional. The elastic component of free energy density of the *N** phase is:

$$F = \frac{1}{2}K_1\left(\vec{\nabla}\cdot\vec{n}\right)^2 + \frac{1}{2}K_2\left(\vec{n}\cdot\vec{\nabla}\times\vec{n} - q_o\right)^2 + \frac{1}{2}K_3\left[\vec{n}\times(\vec{\nabla}\times\vec{n})\right]^2 - \frac{1}{2}\mu_o\Delta\chi H^2, \qquad (1)$$

where $K_{1\text{-}3}$ are the splay, twist and bend elastic constants, respectively, $q_o = 2\pi / p_o$ where p_o is the helical pitch, $\mu_o = 4\pi \cdot 10^{-7} Vs/(Am)$ is the permeability of free space, $\Delta\chi \simeq 10^{-6}$ (SI) is the diamagnetic susceptibility anisotropy, and *H* is the magnetic field.

When a strong enough field $\vec{H} = (0, 0, B/\mu_o)$ is applied along the *z*-axis, the helix becomes unwound with the director pointing everywhere along the field, i.e., $\vec{n} = (0, 0, 1)$. As the field is reduced, the tendency to twist due to the chiral molecular content can compete with the diamagnetic interaction, and below a threshold field [27] $H_t = B_t/\mu_o = (2\pi/p_o)\left(K_2/\sqrt{\mu_o \Delta\chi K_3}\right)$ a heliconical state forms where the director follows an oblique left-handed helicoid, $\vec{n} = (\sin\theta\cos\varphi, \sin\theta\sin\varphi, \cos\theta)$ with a cone angle $\theta > 0$ and $\varphi(x) = 2\pi x/p$. Note that B_t is the highest magnetic field where the the modulated structure with the heliconical director appears, whereas B_1 is the highest magnetic field where the selective reflection is observed experimentally. Since our measurements did not work in UV, where the selective reflection starts, $B_t > B_1$. The tilt angle θ depends on B as $\sin^2\theta = \frac{\kappa}{1-\kappa}\left(\frac{B_t}{B} - 1\right)$ [14], and the heliconical pitch is inversely proportional to the magnetic induction $B = \mu_o H$ [27] as $\frac{p}{p_o} = \frac{\kappa B_t}{B}$, where $\kappa = K_3/K_2$.

If the heliconical pitch is in the UV-VIS-IR range, the material selectively reflects light with peak value $\lambda_p \approx \bar{n} \cdot p$. Here $\bar{n} = \sqrt{(2n_o^2 + n_{e,eff}^2)/3}$, where $n_{e,eff} = \frac{n_e n_o}{\sqrt{n_e^2\cos^2\theta + n_o^2\sin^2\theta}}$ is the average refractive index (n_e and n_o are extraordinary and ordinary refractive index, respectively). The effective refractive index at very small cone angles can be assumed to be field-independent; *i.e.* $\bar{n} \approx n_o$. Under this assumption, the peak wavelength should be inversely proportional to *B*; specifically, $\lambda_p = \frac{\bar{n}}{B}\sqrt{\frac{K_3\mu_o}{\Delta\chi}} = a/B$. As noted above, this prediction is indeed observed, with the coefficient increasing with temperature. This is likely due to the increase of K_3 with *T*, in accord with the independently measured values of elastic constants above the *N*-N_{tb} phase transition [6,7,14,31–33]. Assuming $\bar{n} \sim 1.6$ and $\Delta\chi \sim 5 \cdot 10^{-7}\ SI$, a typical value of $a \approx 4 \cdot 10^3\ nm \cdot T$ gives $K_3 \approx 2.5\ pN$, which compares reasonably well with other determinations of K_3 [6,7,14,31–33].

The width of the peak $\Delta\lambda = \Delta n_{eff} \cdot p$, where $\Delta n_{eff} = n_{e,eff} - n_o$ is the effective birefringence. It clearly increases with decreasing magnetic fields, where the pitch increases, and where θ

increases, i.e., Δn_{eff} is increasing. As M1 could be tuned up to a larger pitch, on average the width of the reflection pitch appears larger, but when comparing the $\Delta\lambda$ of *M1* and *M2* at the same λ_p they are very similar. For small θ the effective birefringence can be approximated as $\Delta n_{eff} \approx \frac{\Delta n(n_e + n_o)}{2n_e^2}\theta^2$. This means that for an ideally field-adjustable heliconical structure with a uniform pitch,

$$\Delta\lambda \approx \frac{\kappa B_t p_o}{B} \cdot \frac{\Delta n(n_e + n_o)\cdot\kappa}{2n_e^2(1-\kappa)}\left(\frac{B_t}{B} - 1\right) \qquad (2)$$

At low magnetic fields when $B << B_t$ this equation predict that $\Delta\lambda \propto 1/B^2$. As can be seen in Figure 4 (b) and (d), this behavior is indeed found experimentally for small B values. Deviations from this behavior are observed only at high magnetic fields.

The observed collapse of the selective reflection at a critical magnetic field B_c is due to the positive local diamagnetic anisotropy of the quasi-nematic order that opposes the increase of the angle between the director and the magnetic field. As explained for the electrically-tuned selective reflection of materials with positive dielectric anisotropy [14], as the field decreases below some critical value that can be recast for the diamagnetic response as $B_c \approx B_t \frac{\kappa\left(2+\sqrt{2(1-\kappa)}\right)}{1+\kappa}$, the heliconical structure, with the axis parallel to the applied field is no longer stable, and transforms into a regular cholesteric right-angle helicoid with the axis being perpendicular to the applied field. Measuring B_t/B_c one therefore can obtain κ. Since we could not measure in the UV range, we could only measure $B_1 < B_t$, thus we can only give an upper limit for $\kappa = K_3/K_2$, which we find to decrease from 0.18 to 0.1 as the temperature decreases from 38ºC to 32ºC. In the case of the *M2* mixture, the upper limit of K_3/K_2 varies from 0.25 to 0.18 from 40ºC to 34ºC, indicating that increasing chiral concentration lead to an increase of κ.

Future experiments will be done in a wider UV-VIS-IR region to be able to measure B_t and B_c. With these we will be able to measure both K_3/K_2 and the cone angle θ.

To summarize, we have demonstrated that magnetic fields can induce a heliconical state in the cholesteric phase of LC dimers above the twist-bend nematic phase, as was predicted long ago. The heliconic state exhibits a wavelength band of reflected light, and this band can be selectively tuned over a wide range from the UV to over 1700 nm in the IR. Measurements of the threshold and critical fields, and of the field-dependent peak positions, can provide the twist to bend elastic constant ratio and the cone angle θ. The ability to tune reflection band using temperature as well as magnetic fields offers intriguing possible applications for novel magneto-optical devices.

Acknowledgement: *This work was financially supported by NSF DMR No. 1307674, NSF DMR-1410378, and AFOSR (FA9550-12-1-0037). The work utilized the facilities of the NHMFL, which is supported by NSF DMR-0084173, the State of Florida, and US Department of Energy.*

5. References

[1] M. Cestari, S. Diez-Berart, D. A. Dunmur, A. Ferrarini, M. R. de la Fuente, D. J. B. Jackson, D. O. Lopez, G. R. Luckhurst, M. A. Perez-Jubindo, R. M. Richardson, J. Salud, B. A. Timimi, and H. Zimmermann, Phys. Rev. E **84**, 31704 (2011).

[2] J. W. Emsley, M. Lelli, A. Lesage, and G. R. Luckhurst, J. Phys. Chem. B **117**, 6547 (2013).

[3] J. W. Emsley, P. Lesot, G. R. Luckhurst, A. Meddour, and D. Merlet, Phys. Rev. E **87**, 40501 (2013).

[4] M. G. Tamba, S. M. Salili, C. Zhang, G. H. Mehl, R. Stannarius, and A. Eremin, RSC Adv. **5**, 11207 (2015).

[5] L. Beguin, J. W. Emsley, M. Lelli, A. Lesage, G. R. Luckhurst, B. A. Timimi, and H. Zimmermann, J. Phys. Chem. B **116**, 7940 (2012).

[6] K. Adlem, M. Čopič, G. R. Luckhurst, A. Mertelj, O. Parri, R. M. Richardson, B. D. Snow, B. A. Timimi, R. P. Tuffin, and D. Wilkes, Phys. Rev. E **88**, 22503 (2013).

[7] V. Borshch, Y.-K. Y.-K. Kim, J. Xiang, M. Gao, A. Jákli, V. P. Panov, J. K. Vij, C. T. Imrie, M. G. Tamba, G. H. Mehl, and O. D. Lavrentovich, Nat. Commun. **4**, 2635 (2013).

[8] V. P. Panov, R. Balachandran, M. Nagaraj, J. K. Vij, M. G. Tamba, A. Kohlmeier, and G. H. Mehl, Appl. Phys. Lett. **99**, 261903 (2011).

[9] V. P. Panov, R. Balachandran, J. K. Vij, M. G. Tamba, A. Kohlmeier, and G. H. Mehl, Appl. Phys. Lett. **101**, 234106 (2012).

[10] S. M. Salili, C. Kim, S. Sprunt, J. T. Gleeson, O. Parri, and A. Jákli, RSC Adv. **4**, 57419 (2014).

[11] S. M. Salili, M.-G. Tamba, S. N. Sprunt, C. Welch, G. H. Mehl, A. Jákli, and J. T. Gleeson, Phys. Rev. Lett. **116**, 217801 (2016).

[12] P. A. Henderson and C. T. Imrie, Liq. Cryst. **38**, 1407 (2011).

[13] V. Panov, M. Nagaraj, J. Vij, Y. Panarin, A. Kohlmeier, M. Tamba, R. Lewis, and G. Mehl, Phys. Rev. Lett. **105**, 167801 (2010).

[14] J. Xiang, S. V. Shiyanovskii, C. Imrie, and O. D. Lavrentovich, Phys. Rev. Lett. **112**, 217801 (2014).

[15] J. Xiang, Y. Li, Q. Li, D. A. Paterson, J. M. D. Storey, C. T. Imrie, and O. D. Lavrentovich, Adv. Mater. **27**, 3014 (2015).

[16] B. Robles-Hernández, N. Sebastián, M. R. de la Fuente, D. O. López, S. Diez-Berart, J. Salud, M. B. Ros, D. A. Dunmur, G. R. Luckhurst, and B. A. Timimi, Phys. Rev. E **92**, 62505 (2015).

[17] I. Dozov, Eur. Lett. **56**, 247 (2001).

[18] D. Chen, J. H. Porada, J. B. Hooper, A. Klittnick, Y. Shen, M. R. Tuchband, E. Korblova, D. Bedrov, D. M. Walba, M. A. Glaser, J. E. Maclennan, and N. A. Clark, Proc. Natl. Acad. Sci. U. S. A. **110**, 15931 (2013).

[19] R. R. R. De Almeida, C. Zhang, O. Parri, S. N. Sprunt, and A. Jakli, Liq. Cryst. **41**, 1661 (2014).

[20] P. K. Challa, V. Borshch, O. Parri, S. N. Sprunt, C. T. Imrie, S. N. Sprunt, J. T. Gleeson, O. D. Lavrentovich, and A. Jákli, Phys. Rev E **89**, 060501 (R) (2014).

[21] E. Gorecka, N. Vaupotič, A. Zep, D. Pociecha, J. Yoshioka, J. Yamamoto, and H. Takezoe, Angew. Chemie **54**, 10155 (2015).

[22] A. Zep, S. Aya, K. Aihara, K. Ema, D. Pociecha, K. Madrak, P. Bernatowicz, H. Takezoe, and E. Gorecka, J. Mater. Chem. C **1**, 46 (2013).

[23] L. Longa and G. Pająk, ArXiv 1511.06792v1 (2015).

[24] R. J. Mandle, E. J. Davis, C. T. Archbold, S. J. Cowling, and J. W. Goodby, J. Mater. Chem. C **2**, 556 (2014).

[25] C. T. Archbold, E. J. Davis, R. J. Mandle, S. J. Cowling, and J. W. Goodby, Soft Matter **11**, (2015).

[26] S. M. Salili, R. R. R. de Almeida, P. K. Challa, S. N. Sprunt, J. T. Gleeson, and A. Jakli, Liq. Cryst., in print (2016).

[27] R. B. Meyer, Appl. Phys. Lett **12**, 281 (1968).

[28] P. G. De Gennes, Solid State Commun. **88**, 1043 (1993).

[29] D. O. Lopez, N. Sebastian, M. R. De La Fuente, J. C. Martinez-Garcia, J. Salud, M. A. Perez-Jubindo, S. Diez-Berart, D. A. Dunmur, and G. R. Luckhurst, J. Chem. Phys. **137**, (2012).

[30] J. Toth, M. D. Bird, S. Bole, and J. W. O'Reilly, IEEE Trans. Appl. Supercond. **22**, 4301604 (2012).

[31] K. L. Atkinson, S. M. Morris, F. Castles, M. M. Qasim, D. J. Gardiner, and H. J. Coles, Phys. Rev. E **85**, 12701 (2012).

[32] C.-J. J. Yun, M. R. Vengatesan, J. K. Vij, and J.-K. K. Song, Appl. Phys. Lett. **106**, 173102 (2015).

[33] R. Balachandran, V. P. P. Panov, J. K. K. Vij, A. Kocot, M. G. G. Tamba, A. Kohlmeier, and G. H. H. Mehl, Liq. Cryst. **40**, 681 (2013).